Molecular simulation study of the curling behavior of the finite free-standing kaolinite layer

Zoltán Ható[a], Jadran Vrabec[b] and Tamás Kristóf[a*]

[a]Department of Physical Chemistry, Institute of Chemistry, University of Pannonia
P.O. Box 158, H-8201 Veszprém, Hungary

[b]Thermodynamics and Process Engineering, Technical University of Berlin,
10587 Berlin, Germany (vrabec@tu-berlin.de)

Abstract

Since kaolinite nanolayers potentially have many important applications, it is crucial to determine the factors that govern their curling behavior. The curling of a single-layer, free-standing kaolinite nanoparticle consisting of nearly 1 million atoms is studied with classical molecular dynamics simulation. Two up-to-date force fields are employed to describe the atomic interactions in the clay. The influence of force field details and of the use of different treatments of interactions (long range correction, potential cut-off radius) on the curling direction is systematically examined. That includes a practically infinite potential cut-off, which means that all atomic interactions are considered explicitly. For every inspected case, the structure is characterized by the overall shape of the particle, the axis of roll-up and particular bond lengths and angles. Both of the two possible curling directions are detected in the present simulations, which contradicts the crystallographic assumption that the constituent tetrahedral sheet can exclusively be on the concave side of curled kaolinite nanolayers.

Keywords: Kaolinite layer, Nanoscroll, Atomistic simulation

*Corresponding author.
E-mail address: kristoft@almos.uni-pannon.hu (T. Kristóf).

1. Introduction

Recent research has focused on the production of 'one-dimensional' layers of kaolinite with a controlled morphology because of their potential applicability in advanced sorption, catalytic and composite materials. Kaolinite layers are constituted by one tetrahedral silica sheet and one octahedral aluminum hydroxide sheet. These layers occur in nature as flat platelets of book-like kaolinite particles, where the platelets are strongly attached to each other by hydrogen bonds. Synthetically separated kaolinite layers tend to curl or form nanoscrolls, in order to minimize the misfit of their tetrahedral and octahedral sheets [1-6]. There is no clear understanding of how this curling process takes place. However, according to crystallographic considerations [7, 8], the tetrahedral sheet is slightly longer than the octahedral one and, in the absence of hydrogen bonds between the layers (i.e., in case of separated layers), the mechanical strain in the structure is released by bending or rolling deformation. It is generally accepted that chains of silica tetrahedrons are more flexible than chains of aluminum hydroxide octahedrons and that the tetrahedral sheet is on the concave (outer) side of such curled nanolayers or nanoscrolls.

All-atom simulations with classical force fields may accurately predict the properties of such materials. Using molecular dynamics (MD), we recently investigated the behavior of a life-sized kaolinite particle model in two different liquids [9]. However, Prishchenko et al. found that even minor differences in simulation parameters, like boundary conditions or cut-off radius of the explicit interaction calculation, can influence whether a free-standing kaolinite nanolayer will roll up with its tetrahedral sheet inside or outside [10]. In the present work, classical MD simulations using two realistic atomic force fields (ClayFF [11] and INTERFACE [12]) were carried out to further examine this issue. Because of theoretical considerations, it was critical to create proper-sized layer models for this study. Artifacts can easily emerge when simulating tiny layers consisting of a few thousand atoms because of the unrealistic ratio of surface atoms to the inner ones. On the other hand, structural changes of kaolinite sheets can remain hidden when a hypothetically infinite layer is constructed by applying periodic boundary conditions in either direction of an atomistic simulation cell with usual size. To ensure that the present simulation results are as realistic as possible and relevant to support experimental studies, life-sized atomic layer models were used.

2. Method

It is known that colloidal kaolinite particles consist of layers with a surface area on the order of at least 10 000 nm^2. Therefore, a free-standing, initially flat kaolinite layer with a size of approximately 100 nm × 100 nm was constructed, specifying the initial atomic positions according to the experimental crystal structure [13]. The composition of the kaolinite unit cell is $Al_2Si_2O_5(OH)_4$, the space group symmetry is C1, and the lattice parameters are a=0.5154 nm, b=0.8942 nm, c=0.7391 nm, α=91.93°, β=105.05°, and γ=89.80°. The layer was built from 200 × 120 doubled unit cells along the crystallographic a and b axes, respectively, which corresponds to 48 000 unit cells and 816 000 atoms (96 000 Al atoms, 96 000 Si atoms, 432 000 O atoms, and 192 000 H atoms). To exclude side-length asymmetry effects, we intentionally restricted ourselves to the square geometry (the angle between crystallographic axes a and b was nearly 90°).

For the interactions between the lattice atoms, the widely used INTERFACE (IFF [12], v1.5 [14]) and ClayFF [11] force fields were employed. These approved classical all-atom force fields are highly accurate for atomic-level modeling of minerals and their interfaces. The fully flexible IFF force field contains quadratic bond stretching and angle bending as well as standard non-bonded Coulombic and 12-6 Lennard-Jones potential terms. By definition, the non-bonded intramolecular interactions are only applied to atom pairs separated by at least three bonds. The ClayFF force field also contains Coulombic and Lennard-Jones potential terms, but considers all possible interatomic interactions (except for the O-H interactions) as being non-bonded. For the unlike Lennard-Jones interactions, the Lorentz-Berthelot combination rule was used.

Canonical MD simulations were performed with the GROMACS program package [15, 16]. The leap-frog integrator was applied with a time step of 1 fs and the temperature was controlled with the Nosé-Hoover thermostat [17]. The non-bonded interactions of the lattice atoms were treated either by (1) a simple potential truncation scheme (PT) with formal periodic boundary conditions and the minimum image convention, or by (2) incorporating standard periodic summation for electrostatics, i.e. Ewald summation. For case (1), the selected (spherical) potential cut-off radius values were multiples of the lattice parameters, i.e., r_{cut} equaled 1×a, 2×a through 4×a and 1×b through 3×b. Furthermore, a very large cut-off radius (r_{cut} = 30 nm) was also applied, which appears to be near the effective range of non-bonded interatomic interactions in such crystal structures. The size of the simulation cell, in the form of a rectangular box, was chosen such that the distance of the kaolinite atoms from the nearest side of the box was larger than the specified cut-off radius. Practically, this resulted in non-

periodic simulations. For case (2), the long-range electrostatic interactions were calculated by the particle mesh Ewald summation method [18] with a real-space cut-off of 1.6 nm. Furthermore, since Ewald summation methods require periodic boundary conditions, 55 nm of vacuum was added to the *a*, *b* and *c* directions on every side of the simulation cell. In this way, a quasi-nonperiodic system was obtained, where the periodic neighbor layers were located farther from the center layer than a layer length.

In addition to the above, there was a conceptually distinct variant of case (1), i.e. simulations were carried out with a direct calculation of all atomic interactions in the kaolinite layer. This was realized by applying r_{cut} = 150 nm, which is larger than the diagonal length of the kaolinite plane, and thus allows for simulations without any potential truncation (noPT). While most MD runs were not much longer than 1 ns and took several days to weeks on a high-performance supercomputer (several hundred processor cores), this last type of runs was extremely demanding, which in turn allowed only far shorter simulations ($\leq$0.1 ns), even though the simulations took months of real time.

For measuring bond lengths and bond angles as well as creating simulation snapshots and movies the Visual Molecular Dynamics program suite [19] was used.

3. Results and Discussion

We studied the formation of curled nanolayers or nanoscrolls at 298 K with MD and primarily analyzed the shapes obtained after around 1 ns of simulation time. The processes themselves were also followed by making movies from simulation snapshots that were saved every 10 ps (for some examples, see Video files 1-3 in Supplementary material). From the latter (and performing some longer runs as well), our observations were twofold. First, as expected, morphological changes of the kaolinite nanolayer had generally not ended within 1 ns, but the characteristic shape was almost reached or could be anticipated. Second, the initial curling direction was typically the same as that detected at the end of the run. After an initial time period, structures in which the curling direction was temporarily ambiguous were rarely observed, and these intermediate shapes could clearly be identified from their typical, microscopically wavy appearance. The final shapes were consistent with those obtained from experiments [4, 5], i.e. curled nanolayers or nanoscrolls were found.

The simulation results for the curling direction, principal bending side of the layer and the formed shape are shown in Table 1. The length of the simulations was around 1 ns, except for the noPT case (~0.1 ns).

Table 1. Simulation results for the curling direction and principal bending side (marked by the name of the crystallographic axes) of the free-standing kaolinite nanolayer, together with snapshots of the formed shapes (the stripe with contrasting color is parallel with the crystallographic *a* axis in the straight plane of the starting layer). The radius of curvature in nm for half-rolled or fully rolled structures is given below the letters code of the bending side (colored background: methoxy-modified layer).

	ClayFF			IFF		
treatment of interac-tions	final layer shape	curling direc-tion*	bending side	final layer shape	curling direc-tion*	bending side
simple cut-off: 0.5154 nm	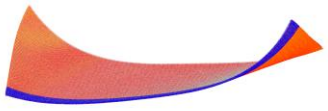	type I	*a*(*b*)	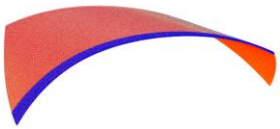	type II	*a*
simple cut-off: 0.8942 nm		type II	*b*(*a*)		type II	*b*
simple cut-off: 1.0308 nm	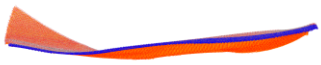	type I	*a*(*b*)		type I	*ab*
simple cut-off: 1.5461 nm	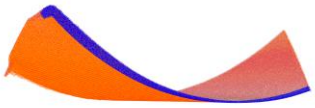	type I	*a*(*b*)	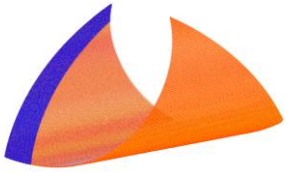	type I	*ab* (~30)
simple cut-off: 1.7884 nm		type I	*ab* (14-17)	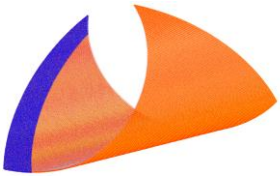	type I	*ab* (~30)
simple cut-off: 2.0614 nm	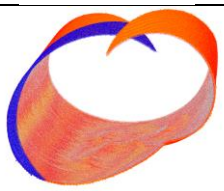	type I	*ab* (15-17)	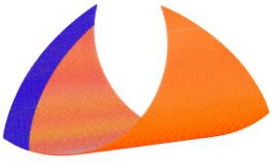	type I	*ab* (~32)

simple cut-off: 2.6826 nm		type I	*b*(*a*) (4-5)	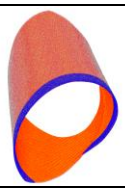	type II	*a*(*b*) (~18)
simple cut-off: 30 nm		type I [§]	*b* (~21)	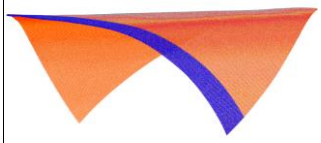	type II	*ab*
				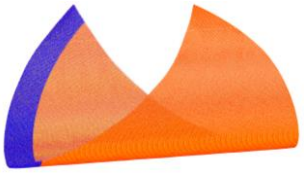	type I[#]	*ab*[#] (~32)
Ewald sum., direct space cut-off: 1.6 nm		type I [§]	*b*(*a*) (16-25)	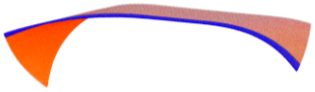	type II	*a*(*b*)
				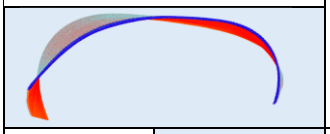	type I[#]	*a*(*b*)[#] (15-21)
non-periodic, without cut-off [¶]		type I	*b*(*a*)	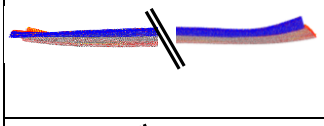	type II	*ab*
				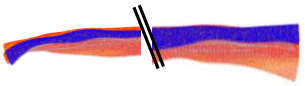	type I[#]	*ab*[#]

[*] Type I and II: kaolinite nanolayer rolls up with the tetrahedral sheet outside or inside, respectively
[#] The literature equilibrium bond length parameter of Si-O bonds was increased by 1.5%
[§] Images have different views, but they are otherwise very similar in shape
[¶] Pairs of black diagonal lines indicate that the middle part is cut out from the picture of the nanolayer

Structures in which the kaolinite layer rolls up with the tetrahedral sheet outside are denoted by type I (which is in agreement with general views) and structures in which the layer rolls up with the tetrahedral sheet inside are denoted by type II. With the ClayFF force field, type I structures were obtained under all conditions, except for the very short cut-off radius r_{cut} = 1×*b*. In the case of the IFF force field, the situation is more complicated, but type II was more dominant among the resulting shapes. For both force fields, there is a clear tendency that the curling direction types are identical for the PT scheme with r_{cut} = 30 nm, for Ewald summation and noPT calculations (this was even the case if the structures produced by the highly time-

consuming noPT simulations were rather platy, with curled-up sides). Consequently, these latter outcomes mutually confirm each other. Because simulations with an explicit calculation of all interactions (noPT) can in this context be considered as approximation-free and yield identical structure types as PT with r_{cut} = 30 nm and Ewald summation, it is highly probable that the application of these latter two, computationally less demanding conditions is sufficient to obtain accurate results. In reverse, the curling directions found in the far shorter noPT calculations with both force fields are probably the final ones. It should be added, however, that in the presence of solvents, Ewald summation gives rise to an induced polarization in such systems due to the artificial periodicity [20]. In our solvent-free but flexible lattice system, this can also lead to small artifacts.

In general, the bending side of the obtained structures can be clearly identified (these are parallel to one of the crystallographic axes *a* or *b*) or the layer starts to roll around the diagonal of the square (*ab*). The structure, or certain parts of the structure, sometimes shows bending along another direction as well. We originally assumed that specific axis preferences of the structural changes might be revealed by selecting r_{cut} values as multiples of the lattice parameters. However, there is no indication from the data in Table 1 for such an effect, especially in case of the IFF force field. It should be noted that PT scheme simulations with r_{cut} = 1×*a* and 1×*b* were taken only for comparison as these cut-off radii are obviously too small for accurate property calculations in crystalline phases with Coulombic interactions.

The curling process appeared to be faster at r_{cut} > 1.5 nm without any axis preference, but it was generally slightly slower with the IFF force field than with the ClayFF one. An exceptional case occurred for the PT scheme with r_{cut} = 2.6826 nm, where the structure obtained with the ClayFF force field had a rather wavy, but otherwise well-recognizable twin-tube form. Its evolution was much faster, leading already after 0.25 ns to tubes with an inner diameter of 8-10 nm on the two opposite ends of the layer. Obviously, if initially larger bending angles in the fringe ranges of the layer enable remote atoms to come closer to each other, approaching bonding distances, this actually accelerates rolling. In this case, the possible interactions of the edge hydroxyl groups with other flexible hydroxyl groups on the same sheet might play a certain role in accelerating the process. Due to the selected layer size, the radius of a perfect single-walled nanotube should be around 17 nm, if the principal roll axis is parallel with one of the crystallographic axes. This, or a slightly larger, radius of curvature applies for most of the half-rolled or fully rolled structures after 1 ns. An occurrence of significantly larger values (around 30 nm) can be attributed to partial rolling or rolling around the diagonal of the layer. Also, there are fully rolled structures that show a small degree of overlap between opposite

layer ends. These (and the existence of the twin-tube-like structure) suggest that such overlaps are energetically favorable and multi-wall nanotube formation cannot be ruled out for lengthier layers.

We found that the simulation results for the formation of curled nanolayers are indeed sensitive to the simulation conditions, such as cut-off radius and long range correction. This finding is in general agreement with the results of a recent elaborate study on this topic [10]. We did not study artificially infinite crystals (even they are infinite in one direction) or the temperature dependence of the rolling process, as these were examined in detail in Ref. [10]. Rather, we concentrated on the less thoroughly tested question of curling direction, using larger kaolinite layers and involving substantial computational resources for higher precision. The problem related to the sensitivity of the curling direction on the treatment of the interactions (cut-off radius and long range correction) can essentially be eliminated by establishing that the type of curling is always the same when using a very large cut-off radius (30 nm), a practically infinite cut-off radius (noPT scheme) or an accurate Coulombic long range correction scheme (Ewald summation), which are the most reliable simulation conditions. However, the two force fields, which have, in general, a proven ability to predict the material properties of kaolinite, behave oppositely in this sense. The sensitivity of the curling direction on the choice of the force field raises concerns, but also offers an opportunity for another explanation: these changes might be sensitive to small effects in real-life situations too. It appears, e.g., that a small modification of the Si-O bonding distance parameters of the IFF force field can yield type I structures instead of type II structures (the ClayFF force field has no such bonding parameters). The corresponding results are depicted in the last three rows of Table 1 (Ewald summation and noPT schemes). In this case, increasing the equilibrium bond length parameters of the Si-O bonds by only 1.5% leads to a complete reversal of the curling direction. According to our experience, the experimental Si-O bond lengths can be relatively well reproduced by the IFF equilibrium bond length parameters for a straight kaolinite plane. However, the final simulation bond lengths are not the same as the equilibrium bond length parameters (they are smaller on average), but are the result of a fine balance of the bonded and non-bonded intramolecular interactions. In a further test, we tried to influence this fine balance by changing the definition concerning the application of the intramolecular non-bonded interactions: instead of ‘three-bonds’ distances, non-bonded interactions were only calculated for atom pairs separated by at least four bonds. Using this somewhat artificial and defective definition, we could repeatedly induce reversals in the curling direction in some cases.

Given the revealed sensitivity to small modifications of the simulation conditions, it is also interesting to examine the solvent effect on kaolinite layer rolling. Introducing only small changes in the present simulation geometry and conditions, our procedure involved grafting of intercalation reagent molecules on the layer surface. For the exfoliation of kaolinite, a series of interdependent intercalation/deintercalation steps are applied and one of the most important reagents that is able to react chemically with the kaolinite surface is methanol. Based on our earlier experimental and theoretical findings [21], we replaced every sixteenth surface hydroxyl group on the octahedral surface of the kaolinite layer by a methoxy group to mimic grafting of methanol. For the methoxy-modified layer, additional MD simulations with normal and increased Si-O bond length parameters using the Ewald summation scheme showed no changes in the basic curling directions (Table 1, second-last row) as compared to the unmodified layer after similar run times. The existence of deviations between the corresponding structures in the roll axis or degree of rolling indicates some biases due to grafting, even if these can partly be attributed to random effects. (Note that some of the present MD runs were repeated using different random initial velocity distributions of the atoms of the clay layer, nonetheless keeping the specified temperature, which convinced us of the reproducibility of the obtained curling directions and basic structures.)

An analysis of changes in terms of the interatomic distances during curling can provide further insight into possible structural deformations of free-standing kaolinite nanolayers. The average adjacent Si-O, Al-O, and Si-Si distances were determined from the final structures. For comparison, these data were also calculated from final simulation structures of a hypothetically infinite, platy kaolinite particle, which was generated from 6 × 4 × 4 doubled unit cells by applying fully periodic boundary conditions. As Table 2 shows, differences of 6-7% between the average Si-O bond lengths of the platy kaolinite particle were obtained with the ClayFF and IFF force fields. Considering that the tested 1.5% increase of the equilibrium bond length parameters of the Si-O bonds generated less than 1% growth in the actual average bond lengths of the platy kaolinite particle (and they are almost zero with bridging O atoms), this clearly indicates that the applied modification of the IFF model parameters was modest. It is remarkable that no notable variations were observed for the average Si-O bond length within the tetrahedral sheet due to curling (as was the case for the average Al-O bond length; data are not presented here). However, for the IFF force field, there seem to be consistent differences between the oppositely curved layers, and for the ClayFF force field, there is a nearly 3% increase of the average Si-O bond length with bridging O atoms as compared to the infinite straight kaolinite plane (in the latter cases the layer rolls up with its tetrahedral sheet outside).

Also, the data in Table 2 reveal consistent though very slight changes in the average adjacent Si-Si distance. The average increase or decrease is minor, since the rolling mechanism lengthens or shortens the Si-Si distances principally along the curling direction.

Table 2. Average adjacent Si-O and Si-Si distances as well as average O-O-O angles in the tetrahedral sheet of the final structures under more reliable simulation conditions, where the ClayFF and the original IFF force fields yield for the free-standing nanolayer type I and type II structures, respectively.

	infinite (periodic) crystal layer		free-standing crystal layer, simple cut-off: 2.6826 nm		free-standing crystal layer, simple cut-off: 30 nm		free-standing crystal layer Ewald sum. (cut-off: 1.6 nm)		free-standing crystal layer non-periodic, without cut-off	
distance / nm	ClayFF	IFF	ClayFF	IFF	ClayFF	IFF	ClayFF	IFF	ClayFF	IFF
Si-O (tetrahedral sheet)	0.157	0.167 0.168[#]	0.156	0.166	0.156	0.167 0.169[#]	0.156	0.167 0.169[#]	0.156	0.167 0.169[#]
Si-O (with bridging O)	0.159	0.163 0.163[#]	0.164	0.163	0.164	0.163 0.163[#]	0.164	0.163 0.163[#]	0.164	0.163 0.163[#]
Si-Si	0.299	0.299 0.299[#]	0.300	0.297	0.300	0.298 0.301[#]	0.300	0.298 0.302[#]	0.300	0.299 0.301[#]
O-O-O angles[*] (tetrahedral sheet)	119.7°	86.4/153.6° 83.9/156.1°[#]	119.8°	84.0/156.0°	119.8°	85.1/154.9° 84.6/155.4°[#]	119.8°	85.2/154.8° 85.3/154.7°[#]	119.8°	85.8/154.2° 84.3/155.7°[#]

[*] β (ClayFF) or β_1/β_2 (IFF); $\alpha = 60°$ in every case (see Fig. 1)

[#] The literature equilibrium bond length parameter of Si-O bonds was increased by 1.5%

Showing no noteworthy changes in the averages, the calculated bond angles (the Si-O-Si or Al-O-Al angle in the tetrahedral or octahedral sheet, respectively, or the Si-O-Al angle) did not give any indication of the curling direction. On the other hand, as we went further into the analysis, the characteristic ring structure of O atoms was examined by determining angles between three neighboring O atoms shared by neighboring silica tetrahedrons. According to the widely accepted experimental crystal structure of kaolinite [13], six interconnected silica tetrahedrons form a regular hexagonal ring with O-O-O angles of 120°. Theoretically, however, this hexagonal arrangement can turn into a ditrigonal one in the actual crystal structure [22]. Interestingly, we observed the presence of this structural change as a dissimilarity between the basic tetrahedral sheet structures produced by the two force fields and not as a result of curling. Whereas the idealized hexagonal arrangement of the O atoms remained with the ClayFF force field, the hexagonal-to-ditrigonal transformation always took place in the simulations with the

IFF force field (cf. Fig. 1 and last row of Table 2). This shrinkage of spacing between the ring atoms seems typical for the IFF force field, independent on the type of curling.

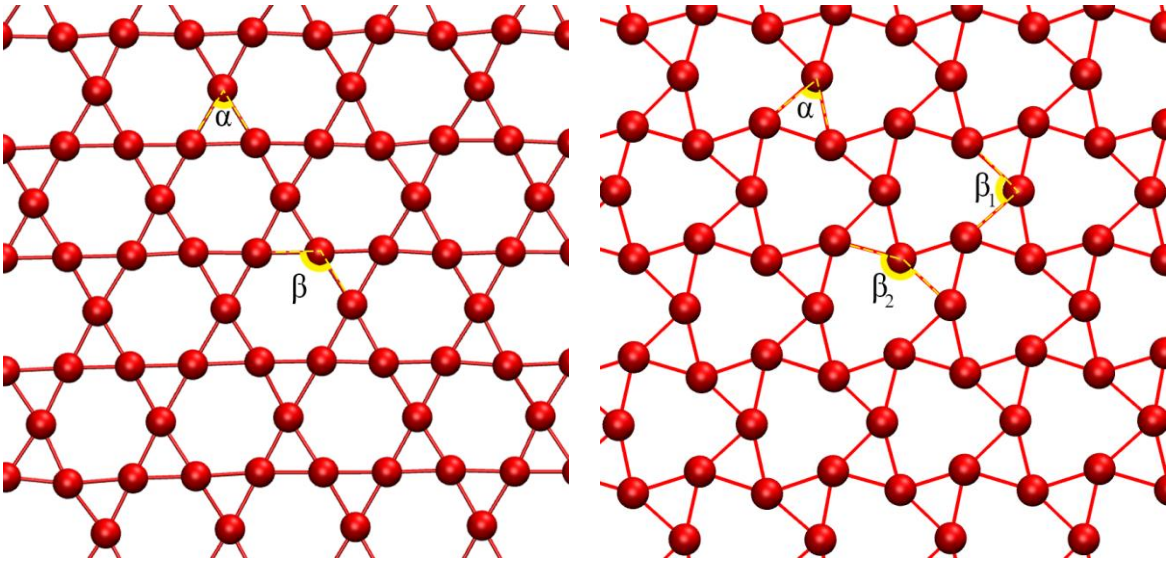

Fig 1. Hexagonal (a) and ditrigonal (b) structures of neighboring O atoms in the tetrahedral sheet of kaolinite layer (note that the lines connecting the atomic spheres are not chemical bonds).

4. Conclusions

The curling behavior of life-sized models of synthetically separated kaolinite nanolayers was studied by classical MD simulations using atomistic force fields with diverse treatments of the calculation of the molecular interactions. Both of the two possible curling directions emerged in the simulations, which contradicts the basic crystallographic, but experimentally not yet verified, assumption that these free-standing nanolayers have a final structure with the tetrahedral sheet outside and the octahedral sheet inside. According to the present findings, this contradiction can be resolved by accounting for potential changes in the Si-O (and consequently other) bond lengths. Furthermore, it was demonstrated that these curled nanolayers or nanoscrolls can exhibit a variety of morphologies, from cylindrical tubes with a roll axis being not parallel with one of the crystallographic axes to structures that show some twist in the layer, with the adjacent Si-Si distance being an indicator of the expanded or shrunken tetrahedral sheet on the outside or inside surface of the curled layer, respectively. However, the investigations revealed a considerable sensitivity of the simulation results on the handling of the interactions

(cut-off radius and long range correction) and the choice of the force field. Several aspects of this phenomenon were examined and the findings raise the possibility that structural changes of real-life, free-standing kaolinite nanolayers can indeed be sensitive to small effects, such as changing the intercalation reagent or the solvent in the exfoliation procedure of kaolinite particles. In this work, we only touched upon the solvent effect on the rolling of the layer by using methoxy-modification and further investigations are needed in this context. There is a large demand for experimental atomic resolution characterization of the structures and crystallographic properties of kaolinite nanolayers under different circumstances [23]. In particular, since these nanolayers can be used, e.g., as an organic catalyst carrier, it would be critical to undoubtedly establish their curling direction or, alternatively, to be able to control the curling process.

From a methodological point of view, we could successfully execute approximation-free MD simulations with respect to the treatment of the interactions in the kaolinite layer (direct calculation of all atomic interactions). In this way, we could determine the most probable curling direction for the given force field and prove that the computationally cheaper particle mesh Ewald summation method with a real-space cut-off of 1.6 nm is sufficient to obtain accurate simulation results. As long as the time- and length-scale problems make quantum chemical simulations of structural changes of such colloidal layers impractical (despite many promising efforts, e.g. Ref. [24]), MD simulations with classical force fields remain the best non-experimental tool for revealing microscopic details. However, for this purpose, extremely reliable force fields are required. Taking into account the difference between the results of the two force fields applied in this work concerning, e.g., the average Si-O bond length and the conceivable, but less probable hexagonal-to-ditrigonal transformation in the tetrahedral sheet with the IFF force field, we can conclude that also these highly realistic force fields need further improvements.

Acknowledgements

Present article was published in the frame of the project GINOP-2.3.2-15-2016-00053 (‘‘Development of engine fuels with high hydrogen content in their molecular structures (contribution to sustainable mobility)”). We gratefully acknowledge the financial support of the National Research, Development and Innovation Office (NKFIH K124353) and the computational support of the Paderborn Center for Parallel Computing (PC2) for providing access to the OCuLUS cluster.

Data availability

The raw/processed data required to reproduce these findings cannot be shared at this time due to technical or time limitations.

References

[1] J.E.F.C. Gardolinski, G. Lagaly, Grafted organic derivatives of kaolinite: II. Intercalation of primary n-alkylamines and delamination, Clay Miner. 40 (2005) 547-556.

[2] S. Letaief, C. Detellier, Clay-polymer nanocomposite material from the delamination of kaolinite in the presence of sodium polyacrylate, Langmuir 25 (2009) 10975-10979.

[3] J. Matusik, E. Wisła-Walsh, A. Gaweł, E. Bielanska, K. Bahranowski, Surface area and porosity of nanotubes obtained from kaolin minerals of different structural order, Clays Clay Miner. 59 (2011) 116-135.

[4] X. Li, Q. Liu, H. Cheng, S. Zhang, R. L. Frost, Mechanism of kaolinite sheets curling via the intercalation and delamination process, J. Coll. Interface Sci. 444 (2015) 74-80.

[5] B. Zsirka, E. Horváth, Zs. Járvás, A. Dallos, É. Makó, J. Kristóf, Structural and energetical characterization of exfoliated kaolinite surfaces, Appl. Clay Sci. 124-125 (2016) 54-61.

[6] É. Makó, A. Kovács, V. Antal, T. Kristóf, One-pot exfoliation of kaolinite by solvothermal cointercalation, Appl. Clay Sci. 146 (2017) 131-139.

[7] B. Singh, I.D.R. Mackinnon, Experimental transformation of kaolinite to halloysite, Clays Clay Miner. 44 (1996) 825-834.

[8] Y. Kuroda, K. Ito, K. Itabashi, K. Kuroda, One-Step Exfoliation of Kaolinites and Their Transformation into Nanoscrolls, Langmuir 27 (2011) 2028-2035.

[9] Z. Ható, G. Rutkai, J. Vrabec, T. Kristóf, Molecular simulation study of kaolinite intercalation with realistic layer size, J. Chem. Phys. 141 (2014) 091102.

[10] D.A. Prishchenko, E.V. Zenkov, V.V. Mazurenko, R.F. Fakhrullin, Y.M. Lvov, V.G. Mazurenko, Molecular dynamics of the halloysite nanotubes, Phys. Chem. Chem. Phys. 20 (2018) 5841-5849.

[11] R.T. Cygan, J.-J. Liang, A.G. Kalinichev, Molecular Models of Hydroxide, Oxyhydroxide, and Clay Phases and the Development of a General Force Field, J. Phys. Chem. B 108 (2004) 1255-1266.

[12] H. Heinz, T.J. Lin, R.K. Mishra, F.S. Emami, Thermodynamically consistent force fields for the assembly of inorganic, organic, and biological nanostructures: the INTERFACE force field, Langmuir 29 (2013) 1754-1765.
[13] D.L. Bish, Rietveld refinement of the kaolinite structure at 1.5 K, Clay. Clay. Miner. 41 (1993) 738-44.
[14] Heinz Laboratory USA, INTERFACE FF 1.5, <http://bionanostructures.com/interface-md>, 2016 (accessed 2016-12-02)
[15] H.J.C. Berendsen, D. van der Spoel, R. van Drunen, GROMACS: A message passing parallel molecular dynamics implementation, Comput. Phys. Commun. 91 (1995) 43-56.
[16] B. Hess, C. Kutzner, D. van der Spoel, E. Lindahl, GROMACS 4: Algorithms for highly efficient, load-balanced, and scalable molecular simulation, J. Chem. Theory Comput. 4 (2008) 435-447.
[17] W.G. Hoover, Canonical dynamics: equilibrium phase-space distributions, Phys. Rev. A 31 (1985) 1695-1697.
[18] T. Darden, D. York, L. Pedersen, Particle mesh Ewald: An N·log(N) method for Ewald sums in large systems, J. Chem. Phys. 98 (1993) 10089-10092.
[19] W. Humphrey, A. Dalke, K. Schulten, VMD: Visual molecular dynamics, J. Molec. Graphics 14 (1996) 33-38.
[20] E. Galicia-Andrés, D. Petrov, M.H. Gerzabek, C. Oostenbrink, D. Tunega, Polarization Effects in Simulations of Kaolinite-Water Interfaces, Langmuir 35 (2019) 15086-15099.
[21] É. Makó, A. Kovács, Z. Ható, T. Kristóf, Simulation assisted characterization of kaolinite-methanol intercalation complexes synthesized using cost-efficient homogenization method, Appl. Surface Sci. 357 (2015) 626-634.
[22] B. Singh, Why does halloysite roll? - A new model, Clays Clay Miner. 44 (1996) 191-196.
[23] É. Makó, I. Dódony, P. Pekker, M. Pósfai, A. Kovács, Z. Ható, T. Kristóf, Nanoscale structural and morphological features of kaolinite nanoscrolls, Appl. Clay Sci. (submitted)
[24] A. Táborosi, R.K. Szilagyi, B. Zsirka, O. Fónagy, E. Horváth, J. Kristóf, Molecular treatment of nano-kaolinite generations, Inorg. Chem. 57 (2018) 7151-7167.